PHYSICS AND CHEMISTRY OF SOLID STATE
V. 26, No. 4 (2025) pp. 858-866
Section: Technology

DOI: 10.15330/pcss.26.4.858-866

Vasyl Stefanyk Carpathian National University

ФІЗИКА І ХІМІЯ ТВЕРДОГО ТІЛА
Т. 26, № 4 (2025) С. 858-866
Технічні науки

UDC: 621.643:620.193

ISSN 1729-4428 (Print)
ISSN 2309-8589 (Online)

N.A. Abd[1], Jawdat Ali Yagoob[2]

Investigation the Effect of Micro and Nano Size (SiO_2) on the Corrosion Resistance of Aluminum

[1]*Kirkuk General Education Directorate-Ministry of Education, Kirkuk, Iraq, Nawal.Ali.Abd@st.tu.edu.iq;*
[2]*Kirkuk Polytechnic College -Northern Technical University, Kirkuk, Iraq, jaw209662@ntu.edu.iq*

This study investigated the effect of nano-SiO_2 (0.125, 0.25, and 0.5 wt %) and micro-SiO_2 (3, 6, and 9 wt %) additions on the corrosion resistance of aluminum (Al) fabricated by powder metallurgy (PM). The Al powder and its composite mixtures were independently ball-milled for 3.5 hrs. at 145 rpm in a 304SS vessel. Green compacts were prepared by uniaxial pressing under 650 MPa, and thereafter sintered at 528 ºC for 0.5h in an electric resistance furnace in an argon atmosphere. The potentiodynamic polarization results showed that the corrosion resistance of the Al-tested samples in a 0.1M HCl solution was improved by the addition of micro- and nano-sized SiO_2 particles. Where, better improvement was detected when micro-sized SiO_2 particles were added. The corrosion resistance of Al was increased by (17.07, 18.24, and 32.49) times when (3, 6, and 9) wt% micro-sized SiO_2 particles were added, respectively. While the addition of nano-sized SiO_2 particles improved the corrosion resistance of Al by (1.79, 2.38 and 6.62) times when (0.125, 0.25 and 0.5) wt% were added. However, the addition of micro- and nano-sized SiO_2 also reduced the pitting corrosion of Al by lifting the E pit of Al to very high potential values when immersed in an acidic solution. These conclusions were obtained from the cyclic polarization results of the samples. Furthermore, XRD and FESEM were utilized to observe, and analyze the structure of the fabricated Al and its composites.

Key words: Aluminum Composites, SiO_2, Electrochemical Corrosion, Powder Metallurgy, HCl Solution.

Received 14 July 2024; Accepted 10 November 2025.

Introduction

Aluminum (Al) is an increasingly important material used in numerous applications. Al is naturally found in nature. Its density is 1/3 of that of steel; thus, it is classified as a light metal [1]. Aluminum composites (AlCs) are mostly used in aerospace zone structural applications, such as helicopter parts (drive shafts, body support for rotor plates, rotor vanes in compressors, and aero-engines), cylinder blocks, drive shafts, brake drums, and cylinder liners [2]. Most commercial researches on metal matrix composites (MMC) have concentrated on using Al and its alloys as the matrix metal because of their combination of light weight, desirable mechanical qualities, and environmental resistance [3].

Powder metallurgy (PM) offers several benefits over other metal-working techniques. This helps producers create products that are more consistent by generating components with a nearly standardized structure, high level of accuracy, and high-quality surface finish [4, 5]. PM is a process of blending fine powdered materials, pressing them into selected shaped parts, and then heating them in a controlled atmosphere to bond the powder [6, 7]. Particulate-reinforced MMC are attractive because of their modest preparation skills, more isotropic properties, and lower cost. Fine and thermally constant ceramic particulates were spread regularly in the matrix, leading to an optimum combination of properties. Therefore, extensive research has been conducted to improve a wide range of alternatives to conventional engineering alloys [8].

AlMCs exhibit improved abilities compared with unreinforced alloys [9]. However, the enclosure of strengthening particles can substantially alter the response of these materials to corrosion, and composites are typically more exposed to corrosion than matrix alloys.

Although the mechanical and physical characteristics of AlCs have been widely investigated, little is known about how AlCs respond to corrosion [10].

The corrosion behavior is a key consideration when evaluating the potential of using composites as structural materials. The physical, tribological, and mechanical characteristics of AlCs have been extensively studied, but systematic examinations of how materials respond to corrosion have been comparatively underfunded [11]. The corrosion resistance of Al and its alloys can be attributed to natural shielding of the oxide layer (passive film) formed on the surface. This oxide film is subject to localized collapse, allowing pitting and crevice corrosion of the underlying substrate, rather than the general corrosion that occurs afterward. Pitting corrosion of Al and its alloys is a specific type that causes small holes or cavities to arise in the material. Because it is more challenging to anticipate, detect, and prevent pitting than a uniform corrosion failure, it is thought to be more damaging. In a massive system, the creation of only one pit can cause the system to disastrously fail [12].

Nervana [13] in a part of her work studied the effect of a 10% HCl solution on the corrosion rate (CR) of SiC and Al_2O_3 reinforced AlCs at four different temperatures using the mass loss method. The CR of Al increased with an increase in the weight fractions of Al_2O_3 and SiC. Ch. Ratnam et al. [14] investigated the corrosion behavior of Al2024 alloy composites prepared with B_4C and graphite powder. The samples were immersed in water: HCl solution with a water-to-HCl ratio of 19:1 for 2 to 10 h. The corrosion of the samples was evaluated using the mass-loss technique. They concluded that the corrosion of Al2024 alloy increased with the addition of B_4C particles. The addition of graphite powder to Al2024-B_4C composites further reduced their corrosion resistance.

Ahmad T. et al [15] part of their research was about effect of SiC content on the corrosion resistance of Al-Mg alloy in 1 M HCl aqueous solution evaluated by mass loss method. They concluded that the addition of SiC particles tends to increase the mass loss of the alloy, and a further increase in the content of the ceramic particles from (5 vol %to 10) vol% led to a further increase in corrosion, particularly after 90 min of exposure to corrosive acidic media.

Munasir et al. [16] studied the CR of Al/ nano-SiO_2 composites prepared via PM, in which two groups of composites were prepared using two different active solutions: N-butanol (B) and tetra-methyl-ammonium hydroxide (T).

The corrosion amounts were detected by potentiodynamic polarization tests in a 1M NaCl medium at room temperature. The CRs for both types of composites, Al/SiO_2 (B) and Al/SiO_2 (T), increased with increasing SiO_2 content. The corrosion resistance of the Al/SiO_2 (T) group was higher than that of the Al/SiO_2 (B) group. Velavan et al. [17] determined the corrosion resistance of Al6061-SO_2 prepared using a stir-casting procedure. They referred to that the corrosion resistance was improved up to 6%.

According to the corrosion results in 3.5 wt. % NaCl solution Mahdavi, S. et al [18] stated that the Co/nano-Al_2O_3 coating deteriorated the corrosion resistance of the Co film. The corrosion current density was increased from 2 to 3 mA cm^{-2} by incorporation of the nanoAl_2O_3-particles, while it was decreased to 0.8 mA cm^{-2} by incorporation of the micro Al_2O_3-particles. On the other hand Ramatouly [19] pointed out in his doctoral dissertation that the most dangerous and common form of localized corrosion in aluminum alloys is pitting corrosion.

It is impossible to predict, and monitor autocatalytic processes owing to the stochastic nature of this phenomenon. Anil Kumar and Vinay Saini [20] investigated the localized corrosion of Al 2024 under fully immersed conditions in 0.25N, 0.50N, 0.75N HCl media using the weight loss method. They referred to the susceptibility of the alloy to intergranular and localized corrosion, and large pits developed within the grains.

Kalenda Mutombo and Madeleine du Toit [21] reported that aluminum 6061 is prone to pitting corrosion in chloride-containing environments. The aluminum-rich matrix adjacent to the $MgSi_2$ intermetallic precipitates or silicon-rich phases formed in Al–Si–Mg alloys has been shown to be susceptible to preferential corrosion. Accordingly, the selection of these alloys to the percent research is a weakness, particularly from the point of view of studying the corrosion behaviors if they are compared with pure Al.

The challenge of the corrosion reduction of Al metal, particularly when made by the PM route, was the motivation to perform the present research to reduce its harmful effects by improving the corrosion resistance with the addition of micro-and nano-sized SiO_2 particles. At the same time, this will enable a comparison between the contribution of different-sized particles to the improvement of the corrosion resistance of Al with the aid of electrochemical phenomena by means of potentiodynamic and cyclic polarization evaluation behavior in dilute aqueous HCl (0.1M HCl) solution for the prepared samples.

I. Experimental Program

Materials and Experimental approach Samples preparation

Al powder supplied by China Jingan Chemicals and Alloy Limited Company with average particle size (APS) 60 μm and its chemical composition is illustrated in the table 1 is used as the matrix metal.

The SiO_2 nanoparticles used were amorphous white, with a particle size of (20-30) nm. In contrast, the APS of the white-colored micro-sized SiO_2 powder was 44 μm. Three groups of samples were prepared using the PM are indicated in table 2. Pure Al powder (group A) was ball-milled by placing the powder and milling balls at a weight ratio of 1:10 in an SS304 vessel for 3.5 hours at 145 rpm [22]. Al-Micro-sized SiO_2 (group B) and Al- nano-sized SiO_2 (group C) were prepared by mixing SiO_2 with Al powder. Then, the sub-groups of both groups (B and C) were ball-milled under the above conditions of milling time and speed. Samples in each group were pressed at 650 MPa.

Table 1.

The chemical composition of the used aluminum powder

Element	Fe	Mn	O	Si	Zn	Cu	Mo	Al
Wt%	0.0003	0.0004	0.0002	0.0002	0.0002	0.0002	0.0002	balance

Table 2.

The prepared Al and its composites groups and subgroups

No		Title of composite	Al Wt%	SiO_2 Wt%
A		Aluminum	100	0
B	1	Aluminum + SiO_2	97	3
	2	Aluminum + SiO_2	94	6
	3	Aluminum + SiO_2	91	9
C	1	Aluminum + SiO_2	99.875	0.125
	2	Aluminum + SiO_2	99.875	0.250
	3	Aluminum + SiO_2	99.500	0.500

The green compact samples were then sintered in an electric resistance furnace (Carbolite type) under an argon gas atmosphere at 528 ºC for 0.5 hour, and then they cooled to room temperature. FESEM and XRD facilities were used for powders and samples microstructure analyses.

II. Electrochemical Measurements

The measurement procedures used for the corrosion tests of Al and its composite sintered samples were performed using potentiodynamic and cyclic polarization methods. A specific holding facility was used to house the electrochemical cell, which consisted of a 300 milliliters beaker with three electrodes submerged in the corrosion solution. All electrodes consisted of an inert platinum auxiliary electrode and an Ag/AgCl/3.5 M KCl type reference electrode. The latter was employed to measure the potential of the working electrode, which was composed of Al and its composite samples with (1± 0.05) cm^2 testing area. Before exposure to the corrosive solution, the two circular parallel faces of the sample were wet-ground using SiC emery papers with grit sizes of 1000, 2000, and 3000. Subsequently, they were polished using a suspension solution of 0.5 µm alumina. Finally, the samples were washed with distilled water and dried in a laboratory oven at 120 °C for ten minutes. The electrochemical cell was coupled to a specialized software interface, which enabled the changes for testing to be recorded on the associated laptop in the form of diagrammatic drawings as well as numerical values. In a 0.1 M HCl aqueous solution, the experiments were carried out at a temperature of 30°C plus or minus one degree Celsius. The corrosion solution was prepared immediately before each examination. The scan rate was set to 1 mV/s. The potential (Ecorr), current density (icorr) of corrosion, and Tafel slopes were measured using the Tafel extrapolation method. The cyclic polarization tests were performed between (+ 3000 and 1500) mV.

III. Results and Discussion

The ratio of surface area to the volume of nano SiO_2 particles with 25 APS is 176 time greater than the ratio of surface area to the volume of micro-SiO_2 with 44 micron APS, if the nano and micro - size particles of SiO_2 are assumed to have either cube or spherical shape. The surface area, volume, and surface area / volume ratio of cube, and spherical shape bodies' formulas are used to obtain the number 176. This fact is true for any shape of added particles. The surface area to volume factor was taken in consideration that compensate the lower wt% nano SiO_2 used to prepare the composite samples with respect to the higher wt% of micro-size SiO_2 used. In other word the surface area to volume factor is more important than the weight percentage when different size particles are used as additions to the metallic matrix.

Initially, little information was available regarding the corrosion behavior of Al/SiO_2 composites fabricated by PM in acidic solutions. Figure.1 illustrates an FESEM image of the Al powder used. The powder particles have a hemispherical configuration. Figures 2 and 3 show the FESEM images of the micro- and nano-sized SiO_2 powders. The micro-sized powder particles had a bulky irregular shape. The nano-powder particles had a spherical shape and agglomerated into large pieces.

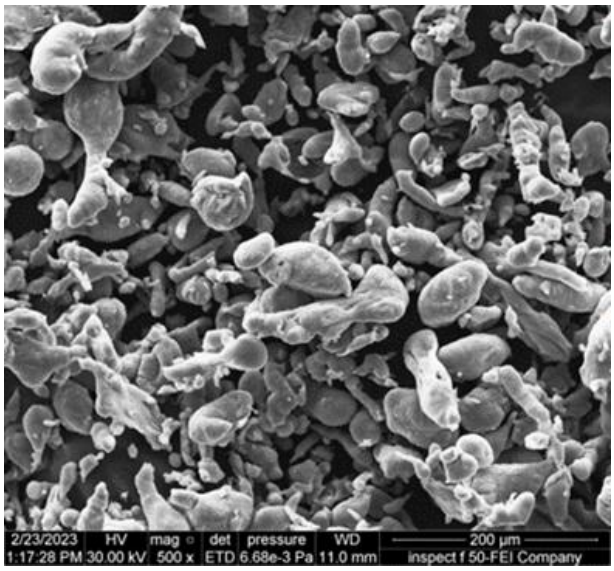

Fig. 1. FESEM photo for Al powder.

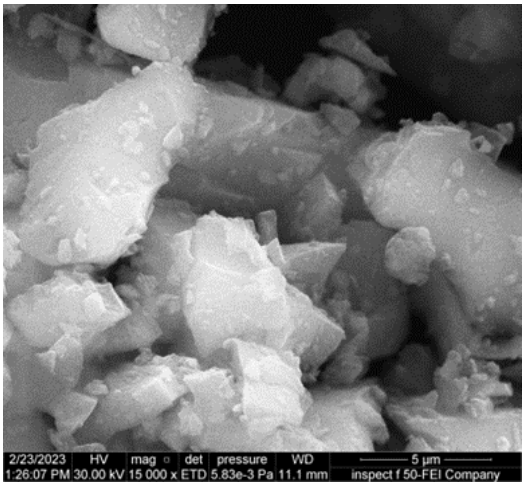

Fig. 2. FESEM photo for micro-size SiO_2 powder.

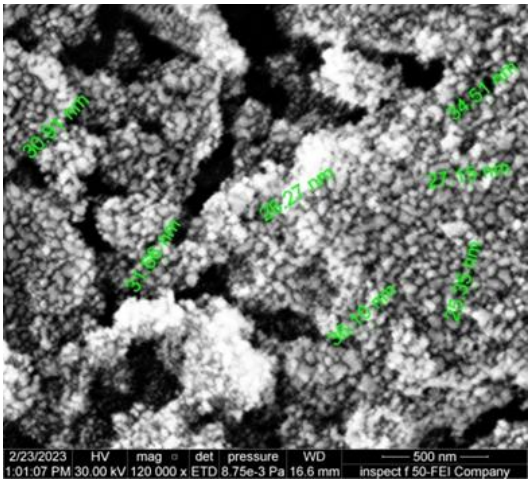

Fig. 3. FESEM photo for nano-size SiO_2 powder.

The XRD patterns of Al and nano- and micro-sized SiO_2 powders are shown in figures 4, 5, 6, and 7. Figure 4 illustrate that there is a good agreement between the XRD patterns of the analyzed Al powder and ICCD card No. (04-0787) and noticeable diffraction peaks were positioned on the curve at 2Θ =38.5 (111), 2Θ =44.7 (200), 2Θ = 65.1 (220) and 2Θ =78.2 (311) [23].

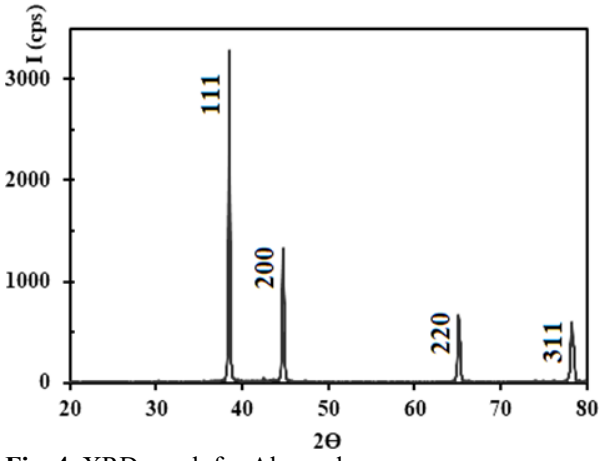

Fig. 4. XRD graph for Al powder.

Changes occurred in the XRD peaks of the Al powder when it was pressed and sintered, as illustrated in figure 5 (A and B). In addition, a deviation of degrees was observed in the characteristic four peaks toward the right hand after pressing and sintering the Al powder. This phenomenon has also reported by A. Rebhi et al [24] and D. Rahmatabadi et al [25] where they are independently and experimentally proved the occurrence of variation in the values of intensity and angle of the characteristic peaks of Al sample according to the effect of heat cycle by annealing, and cold pressing by extrusion or rolling processes.

The XRD patterns for nano-SiO_2 shown in figure 6 indicate that no diffraction peaks were observed, in addition to a broad band centered at 2Θ = 22.7, which is the typical peak for amorphous SiO_2 according to ICCD card No. (29-0085) and the nano-sized SiO_2 powder is amorphous [26]. Micro SiO_2 powder has α-quartz form with a hexagonal crystalline structure, and its XRD spectrum is shown in figure 7. The strong peaks correspond to the spacings of the 100, 101, 110, and 102, crystal planes of quartz SiO_2 and agree well with the ICDD card No. (97631-86-9) [27]. The XRD analysis graphs confirmed the types of utilized powders and their purities (the absence of other substances) because no other phase was found, and there were no contaminating reactions.

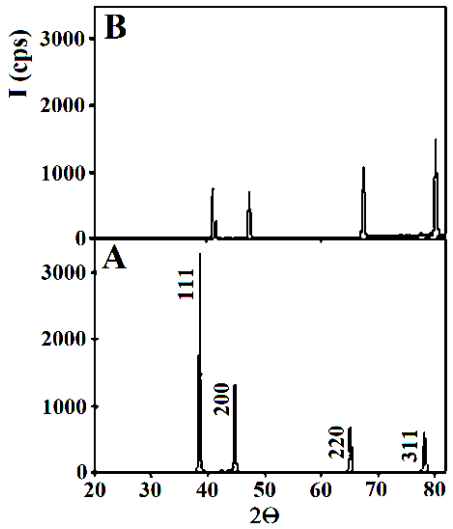

Fig. 5. XRD graph for: A. Al powder, **B.** Sintered Al sample.

Figure 8 explains a FESEM photo for the surface texture of the Al sintered compact sample which is clearly indicates the absence of the porosity on the surface at least at the microstructure level and good bonding between Al particles due to excellent and successful compacting and sintering processes. An observable change is shown in the microstructure of the Al as displayed in the figure 9, where white colored SiO_2 particles are well distributed and imbedded within the Al matrix. For more accurately examination of the surface of the Al-nano-SiO_2 composites, therefore very high magnification power at the substructure level was used. Hence the figure 10 displays the existence of the nano-SiO_2 particles at the Al particles boundaries and within the Al-particles. It is clear that at some positions the Al particles are bonded with each other, while at other position the Al-particles are isolated from each other by a thin (nano-scale) layer of the added nano-SiO_2.

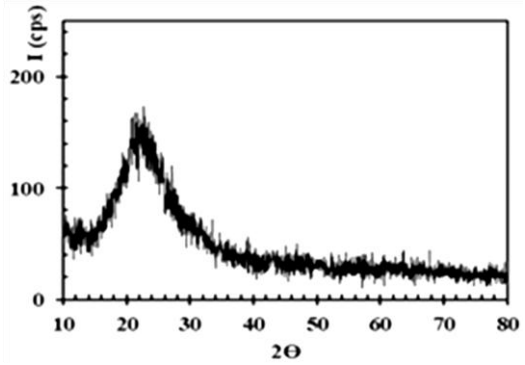

Fig. 6. XRD graph for nano-size SiO_2 powder.

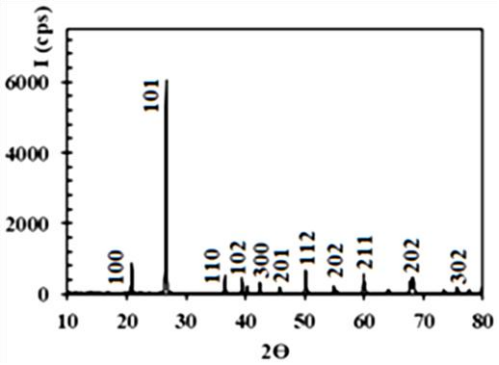

Fig. 7. XRD analysis graph for micro-size SiO_2 powder.

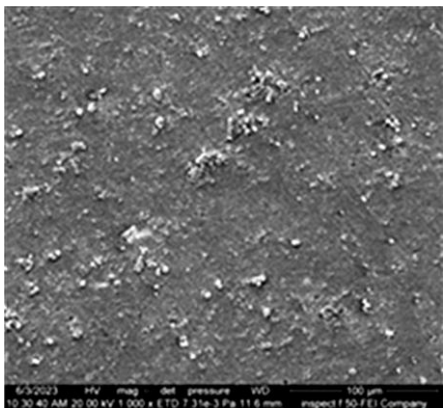

Fig. 8. FESEM photo for Al sintered sample.

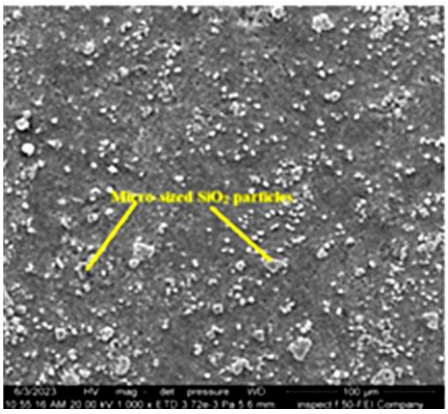

Fig. 9. FESEM photo for Al -micro-SiO_2 composite.

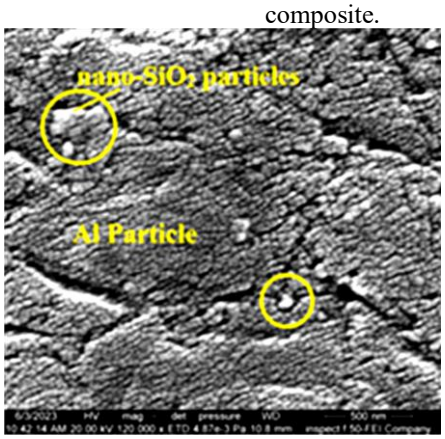

Fig. 10. FESEM photo for Al - nano-SiO_2 composite.

IV. Potontiodynamic Polarization

The anodic polarization curve for the Tafel analysis was determined for a wide range of potentials in volts, as opposed to the corrosion potential (Ecorr) with 1mV/sec scan rate after exposure to the electrolyte. The corrosion parameters, such as the anodic and cathodic Tafel slopes (βa and βc), and corrosion current density (icorr)) were obtained from the polarization curves by Tafel extrapolation. The CRs in millimeters per year were determined with the assistance of the current density of corrosion, which was determined based on ASTM G 102 using the mathematical formula (1) [28].

$$C_R(mpy) = 0.13\frac{e}{\rho} - i_{corr} \quad (1)$$

Where:

C_R: Corrosion rate in mpy = 1 × 0.0254 mmpy.

e: equivalent weight of Al, Al-nano SiO_2 and Al-micro-SiO_2 (gm), and ρ: density of Al, Al-nano SiO_2 and Al-micro-SiO_2 (gm.cm^{-3}).

The Icorr, Ecorr, and Tafel slopes were the primary representations of the findings. In figure 11, the polarization behavior of aluminum sintered compact sample is shown in a solution of 0.1 M hydrochloric acid.

Potentiodynamic and Tafel extrapolation techniques are typically used to evaluate corrosion rate (CR). Even at modest corrosion rates, it is reasonable to identify them [28]. The icorr, Ecorr, and Tafel slopes are listed in table 3. The potentiodynamic polarization curve of aluminum with micro-SiO_2 addition is shown in figure 11, which was constructed under identical conditions as in the previous figure. The icorr and Ecorr values as well as the Tafel slope values derived from the Tafel plots are shown in table 3.

The icorr was enhanced by moving it to lower values when (3, 6, and 9) wt. % micro-SiO_2 added (Groups B–1, 2, and 3). Their values were 6.826×10^{-6}, 6.098×10^{-6} and 3.286×10^{-6} A/cm^2, respectively, compared to 1.145×10^{-4} A/cm^2 for Al-sintered compacts. Hence, CR decreased from 3.239 mmpy for the Al sample to 0.195, 0.177, and 0.0997 for groups B-1, 2 and 3 samples.

The potentiodynamic polarization curve of aluminum with nano-SiO_2 addition is shown in figure 12. This curve was examined under conditions identical to those used for the aluminum-sintered compact sample. The icorr, Ecorr, and Tafel slope values acquired from the Tafel plots are listed in Table 3. These values were derived from Tafel lines. The icorr was improved by shifting it to lower values at (0.125, 0.25 and 0.5) wt% nano-SiO_2 (Group C- 1, 2 and 3 respectively). Their values were 6.386×10^{-5}, 4.795×10^{-5} and 1.726×10^{-5}A/cm^2, respectively, as compared to 1.145×10^{-4} A/cm^2 for the Al-sintered compact sample. Hence, the CR decreased from 3.239 mmpy for the Al sample to 1.807, 1.357, and 0.489 for the samples of groups C-1, 2 and 3 samples, respectively, as shown in figure 12.

However, the CR results showed that the addition of micro- and nano-SiO_2 was useful because it improved corrosion resistance at all addition amounts for both sizes, particularly at the highest amount of addition. But the micro sized - SiO_2 was more active than nano-sized one in its contribution to reducing the CR of Al. The practical and logical explanation for these results could be the isolation characteristic that the SiO_2 particles played by creating a barrier between the Al particles and the corrosive acidic solution in noticeable areas at the Al particle surfaces and Al particles boundaries, thus lowering the dissolution of Al, which is reflected positively in the improvement of the corrosion resistance of Al. The results of the present research were in good agreement (from point of view added particle size) with the work of Loto, Roland Tolulope et al [29] where they are concluded that aluminum matrix composite containing 500 nm alumina particles has better corrosion resistant than the composite containing 80 nm particle size alumina in 0.1M H_2SO_4 and 1.78% NaCl solution, according to their potentiodynamic polarization tests results. On other hand Mahdavi, S and his co-workers [18] in a part of their work were calculated electrochemical parameters about the effect of alumina particle size on corrosion behavior of Co/Al_2O_3 composite coatings and their results confirmed that the incorporation of micro-sized alumina particles within the cobalt matrix has the greatest effect on increasing the corrosion resistance than nano-alumina addition. Their conclusion is in well agreement with the result of the present work.

The lower corrosion resistance improvement took place when nano-size SiO_2 particles used with respect to the higher corrosion resistance improvement that took place when micro-size SiO_2 particles used could be due to lager amount of voids that associated the preparation of Al / nano-size SiO_2 composites. Where, these voids provided easy ways for the corrosive HCl solution to reach the metal surface.

V. Cyclic Polarization

Cyclic polarization is extremely useful system for

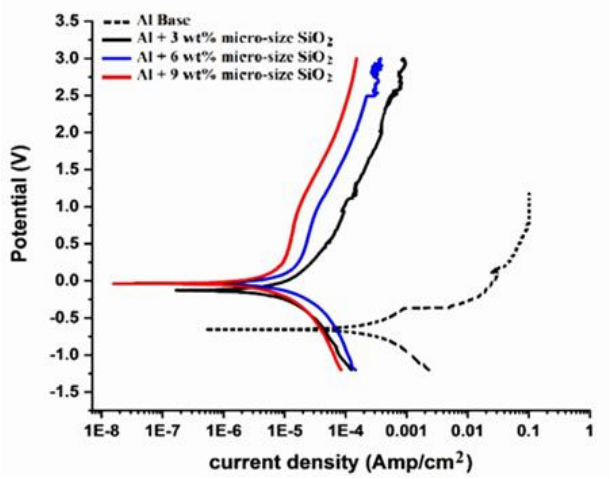

Fig. 11. . Potontiodynamic polarization of Al - micro-SiO_2 composite

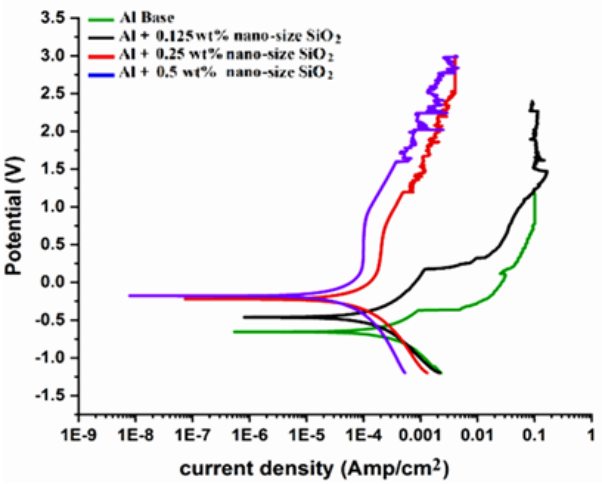

Fig. 12. Potontiodynamic polarization of Al - nano-SiO_2 composite.

Table 3.

Some obtained data from potontiodynamic and cyclic polarization tests

No	Group		I_{corr} (A/cm^2)	-E_{corr} (V)	βa(V/dec)	-βc (V/dec)	E pit V	CR mmpy
1	A		1.145×10^{-4}	0.652	0.208	0.194	-376	3.239
2	B	1	6.826×10^{-6}	0.130	0.204	0.203	Nil	0.195
3		2	6.098×10^{-6}	0.048	0.194	0.230	Nil	0.177
4		3	3.286×10^{-6}	0.0402	0.181	0.230	-	0.0997
5	C	1	0.386×10^{-5}	0.459	0.197	0.203	Nil	1.807
6		2	4.795×10^{-5}	0.205	0.199	0.214	Nil	1.357
7		3	1.726×10^{-5}	0.186	0.197	0.222	1.601	0.489

defining the susceptibility of metallic materials to pitting [28, 30]. Figure 13 shows that the apex potential for the Al sample is 3000 mV. The backward opposing scan curve begins to the right of the forward scan, which means that it begins to move in the direction in which a larger current density is experienced. Documentation indicates that this behavior that Al has low resistivity to local corrosion [28, 30]. This behavior establishes that breakdown of the oxide film occurred, particularly at −0.376 V, as listed in table 3. Accordingly the test is ensured that the Al sample was subjected to pitting under test conditions.

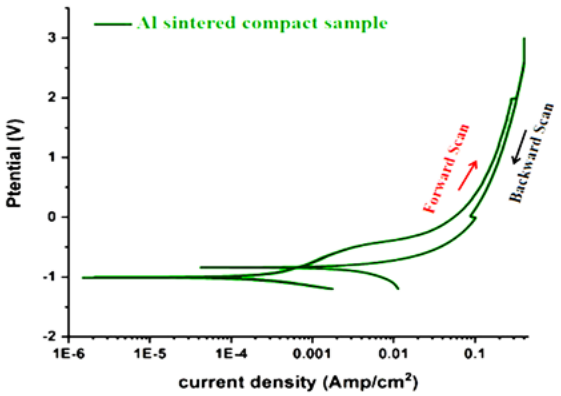

Fig. 13. Cyclic polarization of Al sintered compact sample**.**

At the same scan rate and potential range the addition of 9 wt% micro-SiO_2 particles addition improved the pitting resistance, where E pit is disappeared and no loop was formed between the forward and reverse scans, which insured the absence of the pitting corrosion for this type of Al-SiO_2 composite. This is well clarified in the figure 14. The same improvement occurred when 0.5 wt% nano-SiO_2 particles were added to Al as indicated in the figure 15, by raising E pit value from (- 0.376 to 1.601) Volt. The above cyclic polarization test results explained the benefit of the addition of micro and nano-sized SiO_2 toward the improvement of the resistance for Al both against general and pitting corrosion of Al a 0.1 M HCl solution, which was selected for the present study because it is an effective solution for validating both general and localized corrosion of metals and alloys, that show passivity behavior such as Al.

For a clearer understanding of the effects of micro- and nano-size SiO_2 additions on the corrosion behavior of Al by means of cyclic polarization, beside to the data of E pit indicated in the table 3, the combination of cyclic polarizaition curves for both sizes SiO_2 additions to the Al (groups B and C samples) are gathered and compared with that of pure Al sample (group A) as shown in the figures 16 and 17, respectively. The highest addition amount for both micro- and nano-sized SiO_2 additions moved the curve to the right and E corr to a more positive value, which is strong evidence of the improvement in Al resistance against localized (pitting) corrosion by manufacturing the composite material with SiO_2 addition by PM process.

Conclusions

1. The absence of the porosity from the prepared Al and its composites at least at the microstructure level

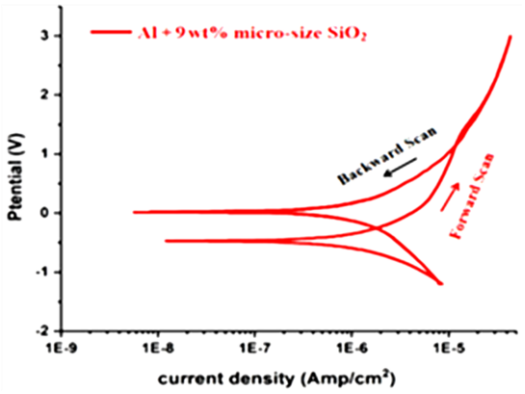

Fig. 14. Cyclic polarization of Al- 9 wt% micro SiO_2 composite sample.

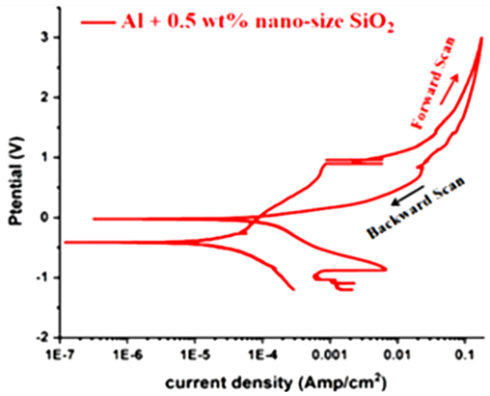

Fig. 15. Cyclic polarization of Al- 0.5 wt% nano SiO_2 composite sample.

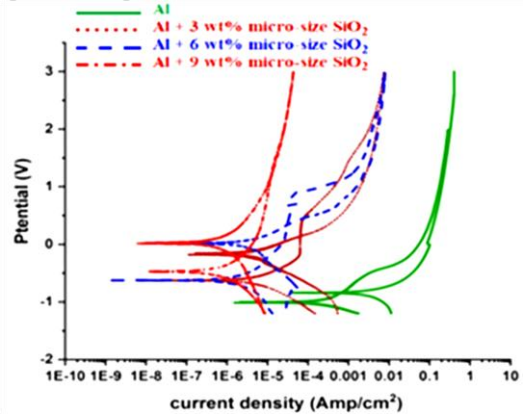

Fig. 16. Cyclic polarization of Al-nano SiO_2composites (group B) samples.

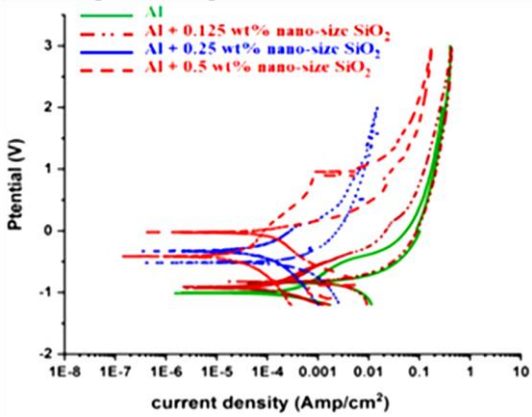

Fig. 17. Cyclic polarization of Al-nano SiO_2 composites (group C) samples.

prove the success of the PM steps performed.

2. The addition of the both micro and nano-sized SiO_2 particles were improved the general corrosion of Al in 0.1 M HCl solution, where the greatest improvement was 32.49 times at 9 wt% micro-size SiO_2 addition. On other hand the greater improvement of corrosion resistance was 6.62 times at 0.5 wt% nano-sized SiO_2 addition.

3. The cyclic polarization results explained the beneficial effect of the micro- and nano-sized SiO_2 additions in improving the pitting corrosion resistance of Al against a 0.1 M HCl solution in the absence of an E pit for the Al-9wt% micro-sized SiO_2 composite, and lifting up its value for Al-0.5 wt% nano-sized SiO_2 composite with respect to that of Al sintered compact with no addition.

4. It is important to note that the addition of 9 wt% micro-sized particles tends to collapse the loop formed between the forward and reverse cyclic polarization scans, which ensures the absence of pitting corrosion for this type of Al-SiO_2 composite.

Abd N.A. – Doctor of Physics/ Solid Physics, Lecturer at Kirkuk General Education Directorate.

Yagoob Jawdat Ali – Doctor of Metallurgy Engineering -Nanomaterials, Professor at Kirkuk Polytechnic College, Northern Technical University. Coressponding Auothor

[1] Kadir Gundogan, Dilan Koksal, Alperen Refik Bilal Özsari, *A Study on Corrosion Behaviour of Different Al Matrix Composi*tes, Journal of Science and Technology, 8(2), 9 (2018).

[2] Muna Khethier Abbass, Mohammed Abdulateef Ahmed, *Study of Erosion- Corrosion Behavior of Aluminum Metal Matrix Composite*, Eng. & Tech. Journal, 32(3), 406 (2014); https://doi.org/10.30684/ETJ.32.3B.3.

[3] B. Bobic, S. Mitrovic, M. Babic, I. Bobic, *Corrosion of Metal-Matrix Composites with Aluminium Alloy Substrate*, Tribology in industry, 32(1), 3 (2010).

[4] A. Panda, J.Dobransky, M. Jancik, I. Pandova, M. Kacalova, *Advantages and Effectiveness of the Powders metallurgy in Manufacturing Techniques*, metallurgy ,57 (4), 353 (2018).

[5] Mikell. P. Groover, *Fundamentals of Modern Manufacturing Materials, Processes, and Systems*, Fifth Edition (2012), USA.

[6] M. Meignanamoorthy, *Synthesis of Metal Matrix Composites via Powder Metallurgy Route: a Review* Mechanics and Mechanical Engineering, 22 (1), 65 (2018); https://doi.org/10.2478/mme-2018-0007.

[7] Bhaskar Raju S A1, A R K Swamy and A Ramesh, *Mechanical and Tribological Behaviour of Aluminium Metal Matrix Composites Using Powder Metallurgy Technique-A Review Int*. J. Mech. Eng. & Rob. Res., l3(4), (2014); http://13.232.72.61:8080/jspui/handle/123456789/457.

[8] Venkateswarlu, A. K. Ray, S. K. Chaudhury and L. C. Pathak, *Development of Aluminium Based Metal Matrix Composites*. National Metallurgical Laboratory, Jamshedpur - 831007, 171(2002).

[9] Ileana Nicoleta Popescu, Simona Zamfir, Violeta Florina Anghelina, and Carmen Otilia Rusanescu, *Processing by P/M route and characterization of new ecological Aluminum Matrix Composites (AMC)*, International Journal of Mechanics, 4 (3), 43(2010).

[10] I. Gurrappa, V. V. Bhanu Prasad, *Corrosion characteristics of aluminium based metal matrix composites*, Materials Science and Technology, 22 (1), 115 (2013); https://doi.org/10.1179/174328406X79324.

[11] H.M. Zakaria, *Microstructural and corrosion behavior of Al/SiC metal matrix composites*, Ain Shams Engineering Journal, 5, 831 (2014); https://doi.org/10.1016/j.asej.2014.03.003.

[12] H. M. Nykyforchyn, O. T. Tsyrulnyk, O. I. Zvirko, N. V. Kret, *Damage of materials during operation, methods of its diagnosis and forecasting*, Proceedings of the International scientific and technical conference, 80 (2019).

[13] Nervana A. Abd Alameer, *Studying the Effect of Chemical Solution on Corrosion Behavior of SiC and Al_2O_3 Reinforced Aluminum Composite Materials*, Eng. & Tech. Journal, 29(15), 3194 (2011).

[14] Ch. Ratnam, K. Sunil Ratna Kumar, *Corrosion Behaviour of Powder Metallurgy Processed Aluminium Self Lubricating Hybrid Metal Matrix Composites with B_4C and Gr Additions*, International Journal of Mechanical Engineering, 279 (2017).

[15] Ahmad T. Mayyas, Mohammad M. Hamasha, Abdalla Alrashdan, and others, *Effect of Copper and Silicon Carbide Content on the Corrosion Resistance of Al-Mg Alloys in Acidic and Alkaline Solutions*, Journal of Minerals & Materials Characterization & Engineering, 11(4), 335(2012); https://doi.org/10.4236/jmmce.2012.114025.

[16] Munasir, Triwikantoro, Mochamad Zainuri, Ralph Bäßler, and Darminto, *Mechanical Strength and Corrosion Rate of Aluminium Composites (Al/SiO_2): Nanoparticle Silica (NPS) as Reinforcement*, Journal of Physical Science, 30(1), 81(2019); https://doi.org/10.21315/jps2019.30.1.7.

[17] K. Velavan, et al. *Determination of Corrosion Resistance Properties of Al-SiO_2 Composite Material*. Journal of Physics: Conference Series. 2070 (1), 012191 (2021); https://doi.org/10.1088/1742-6596/2070/1/012191.

[18] S. Mahdavi, A. Asghari-Alamdari, M. Zolola Meibodi, *Effect of alumina particle size on characteristics, corrosion, and tribological behavior of Co/Al_2O_3 composite coatings*. Ceramics International, S0272884219331670 (2019); https://doi.org/10.1016/j.ceramint.2019.10.28.

[19] Ramatouly, *Processing and microstructure effects on the strength and the localized corrosion resistance of ultra-fine grained al-mg-si alloys*, Doctoral Dissertation, Texas A&M University, 33 (2019); https://hdl.handle.net/1969.1/188771.

[20] Anil Kumar and Vinay Saini, *An investigation of localized corrosion of Al2024 under fully immersed condition of chloride (HCl) media*, International Journal of Mechanical and Production Engineering Research and Development (IJMPERD) 7(4), 291(2017); https://doi.org/10.24247/ijmperdaug201729.
[21] Kalenda Mutombo; Madeleine du Toit. *Corrosion fatigue behaviour of aluminium alloy 6061-T651 welded using fully automatic gas metal arc welding and ER5183 filler alloy*., International Journal of Fatigue, 33(12), 1539 (2011); https://doi.org/10.1016/j.ijfatigue.2011.06.0.
[22] Jawdat Ali Yagoob, Muna Khethier Abbass, *Characterization of Cobalt Based CoCrMo Alloy Fabricated by Powder Metallurgy Route*, 2nd International Conference for Engineering, Technology and Science of Al-Kitab University, (2018); https://doi.org/10.1109/ICETS.2018.8724615.
[23] Jo´zsef Petro, La ´szlo´ Hegedu˝s, Istva´n E. Sajo, *A new, aluminium oxy-hydrate supported NiAl skeleton catalyst,* Applied Catalysis A: General 308, 50 (2006); https://doi.org/10.1016/j.apcata.2006.04.004.
[24] A. Rebhi; T. Makhlouf; N. Njah. X-Ray diffraction analysis of 99.1% recycled aluminium subjected to equal channel angular extrusion. , 2(3), 1263 (2009); https://doi.org/10.1016/j.phpro.2009.11.090.
[25] D. Rahmatabadi, R. Hashemi∗, B. Mohammadi, T. Shojaee, *Experimental evaluation of the plane stress fracture toughness for ultra-fine grained aluminum specimens prepared by accumulative roll bonding Process,* Materials Science & Engineering A 708, 301(2017); http://dx.doi.org/10.1016/j.msea.2017.09.085.
[26] PY Jia1, XM Liu1, GZ Li, M Yu, J Fang and J Lin, *Sol-gel synthesis and characterization of SiO_2@$CaWO_4$,SiO_2@$CaWO_4$:Eu^{3+}/Tb^{3+} core-shell structured spherical particles*, Institute of Physics Publishing, Nanotechnology, 17, 734 (2006); https://doi.org/10.1088/0957-4484/17/3/020.
[27] Marlene C. Morris, Howard F. McMurdie, Eloise H. Evans, Boris Paretzkin, Harry S. Parker, and Nicolas C. Panagiotopoulos, *Standard X-ray Diffraction Powder Patterns Section 18*, International Centre for Diffraction Data, National Measurement Laboratory National Bureau of Standards Washington, DC 20234, (1981).
[28] Muna K. Abbass, Jawdat A. Yagoob, *Corrosion Behavior and Mechanisms of Co-Cr-Mo Alloy Fabricated by Powder Metallurgy Route in Ringer's Solution*, Tikrit Journal for Dental Sciences 7(1), 11 (2023); https://doi.org/10.25130/tjds.7.1.2.
[29] Loto, Roland Tolulope; Babalola, Phillip. *Effect of alumina nano-particle size and weight content on the corrosion resistance of AA1070 aluminum in chloride/sulphate solution*. Results in Physics, 10, 731 (2018); https://doi.org/10.1016/j.rinp.2018.07.025.
[30] Muna Khethier Abbass, Jawdat Ali Yagoob, *Influence of Al_2O_3 Nanoparticles on the Corrosion Behavior of Biomedical CoCrMo Alloy in Ringer's Solution*, AIP Conference Proceedings 2787, 020003 (2023); https://doi.org/10.1063/5.0150065.

Н.А. Абд[1], Джавдат Алі Ягуб[2]

Дослідження впливу мікро- та нанорозмірного SiO_2 на корозійну стійкість алюмінію

[1]*Управління загальної освіти м. Кіркук, Міністерство освіти, м. Кіркук, Ірак, Nawal.Ali.Abd@st.tu.edu.iq;*
[2]*Інженерно-технічний коледж Кіркука, Північний технічний університет, м. Кіркук, Ірак, jaw209662@ntu.edu.iq*

У роботі досліджено вплив добавок нанорозмірного SiO_2 (0,125; 0,25 та 0,5 мас. %) і мікророзмірного SiO_2 (3; 6 та 9 мас. %) на корозійну стійкість алюмінію (Al), виготовленого методом порошкової металургії. Порошок Al та композитні суміші окремо піддавали кульовому помелу протягом 3,5 год при швидкості 145 об/хв у посудині з нержавіючої сталі 304SS. «Зелені» пресовки формували методом одновісного пресування при тиску 650 МПа, після чого спікали при температурі 528 °C протягом 0,5 год в електричній муфельній печі в атмосфері аргону.

Результати потенціодинамічної поляризації показали, що корозійна стійкість досліджуваних зразків Al у 0,1М розчині HCl підвищується при введенні як мікро-, так і нанорозмірних частинок SiO_2. При цьому більш істотне покращення спостерігалося у випадку використання мікророзмірного SiO_2. Корозійна стійкість Al зростала у (17,07; 18,24 та 32,49) раза при додаванні відповідно (3; 6 та 9) мас. % мікророзмірного SiO_2. Водночас додавання нанорозмірного SiO_2 підвищувало корозійну стійкість у (1,79; 2,38 та 6,62) раза при вмісті (0,125; 0,25 та 0,5) мас. %. Також введення мікро- та нанорозмірного SiO_2 зменшувало пітингову корозію Al за рахунок зміщення пітингового потенціалу до більш високих значень в умовах дії кислого середовища. Такі висновки отримано за результатами циклічної поляризації зразків. Крім того, для аналізу структури виготовлених зразків Al та його композитів було використано методи рентгеноструктурного аналізу (XRD) та сканувальної електронної мікроскопії з польовою емісією (FESEM).

Ключові слова: алюмінієві композити, SiO_2, електрохімічна корозія, порошкова металургія, розчин HCl.